



ELSEVIER

Journal of Crystal Growth 174 (1997) 424–433

JOURNAL OF **CRYSTAL GROWTH**

# Growth morphologies of heteroepitaxial rutile films on sapphire substrates

P.A. Morris Hotsenpiller<sup>a,\*</sup>, A. Roshko<sup>b</sup>, J.B. Lowekamp<sup>c</sup>, G.S. Rohrer<sup>c</sup>

<sup>a</sup> DuPont Company, Experimental Station, Wilmington, Delaware 19880-0356, USA

<sup>b</sup> National Institute of Standards and Technology, Boulder, Colorado 80303-3328, USA

<sup>c</sup> Department of Materials Science and Engineering, Carnegie Mellon University, Pittsburgh, Pennsylvania 15213, USA

## Abstract

The growth morphologies of (1 0 0), (1 0 1) and (0 0 1) rutile films grown on sapphire substrates by the ion-beam sputter deposition technique have been examined as a function of film/substrate orientation, film thickness, substrate surface preparation, growth rate and growth temperature. The rutile films of each orientation appear to grow via island (Volmer–Weber) type growth. At the early stages of growth ( $\leq 100$  Å) on as-polished substrates, the roughnesses of the films grown at 725°C and 3 Å/min are correlated to their lattice mismatches and inversely related to the calculated surface energies of their sapphire substrates. Thicker films ( $\geq 700$  Å) have morphologies which are orientation dependent, appear to minimize their surface energies and are stable with respect to annealing. Rougher and slightly less crystallographically aligned (1 0 0) and (0 0 1) rutile films result from the more three-dimensional growth found on annealed sapphire substrates. Relatively small increases in the growth rate, at very low rates, can change the details of the surface structures present. The changes in the morphologies observed on films grown at lower temperatures indicate that the processes controlling their development have a strong temperature dependence at all stages. Comparisons were also made between (1 0 0) and (1 0 1) rutile films grown by the ion-beam sputter deposition and metalorganic chemical vapor deposition techniques under similar conditions. The chemical vapor deposited films have morphologies which are similar to the ion-beam sputtered films with comparable thicknesses, but grown at lower temperatures.

PACS: 61.16.Ch; 68.35.Bs; 68.55. – a; 81.05.Je; 81.15.Cd; 81.15.Gh

Keywords: Titanium dioxide; Rutile; Films; Epitaxy; Morphologies; Growth; Sputtering; MOCVD

## 1. Introduction

Crystalline TiO<sub>2</sub> thin films are of interest for use in a range of applications including photocatalysts

for wastewater treatment, atmospheric pollution control and solar energy conversion, as well as gas sensors, waveguides, and as components in a variety of electronic devices. This interest has led to research into growth techniques for producing TiO<sub>2</sub> films. While polycrystalline films are sufficient for many uses, there are potential benefits to using

\* Corresponding author. Fax: + 1 302 695 1664; e-mail: morrispa@esvax.dnet.dupont.com.

epitaxial films for some applications. Heteroepitaxial  $\text{TiO}_2$  has been grown by a variety of techniques including ion-beam sputter deposition (IBSD) [1], chemical vapor deposition (CVD) [2, 3], metalorganic chemical vapor deposition (MOCVD) [4–8] and the reactive-ionized cluster-beam technique (RICB) [9–11]. Several orientations of the high temperature rutile and low temperature anatase phases have been grown.

The electrical and optical properties of  $\text{TiO}_2$  make it attractive for many of these applications. However, the surface morphology is also important in determining its properties for several uses. The evolution of surface morphologies during heteroepitaxial growth of semiconductor films is receiving an increased level of attention [12]. Unfortunately, the growth mechanisms and morphology development in heteroepitaxial oxide systems have only rarely been examined and are not at all well understood. In this paper, we report the results of our research on the growth mechanisms and morphology development of heteroepitaxial rutile films on single crystal  $\text{Al}_2\text{O}_3$  (sapphire) substrates. The surface morphologies of rutile films grown by the IBSD technique are examined as a function of film/substrate orientation, film thickness, substrate surface preparation, growth rate and growth temperature. Comparisons are also made between films grown by the IBSD and MOCVD techniques under similar conditions.

## 2. Experimental procedure

$\text{TiO}_2$  films were grown using the IBSD and MOCVD techniques, as described in Refs. [1, 4]. The IBSD technique was implemented using a system developed to produce complex oxide thin films. The vacuum chamber was evacuated to  $1 \times 10^{-7}$  Torr prior to deposition and the substrates were introduced into the system through a load-lock chamber. The substrate stage was heated by halogen lamps and the temperature was monitored by a thermocouple and an infrared pyrometer. Deposition resulted from reactively sputtering a high-purity (99.995%) Ti target with a Xe-ion beam from a 3 cm Kaufmann-type ion source. The ion-beam energy and current were

1000 eV and 20 mA, respectively. The growth atmosphere consisted of  $1 \times 10^{-4}$  Torr of Xe and  $1 \times 10^{-4}$  Torr of  $\text{O}_2$ . Films were grown at substrate temperatures from 450–725°C. The growth rate varied between 3 and 7 Å/min. Relatively slow growth rates were used in this work so that the structures observed would be as close to equilibrium as possible. Films were grown with thicknesses in the range of 15–4500 Å to examine their growth mechanisms and morphology development.

The MOCVD films were grown using a solid metalorganic precursor, tris(2,2,6,6-tetramethyl-3,5-heptanedionato) titanium (III) ( $\text{Ti}(\text{TMHD})_3$ ) in an inverted pedestal, hot-walled reactor. The base pressure of the reactor was  $1 \times 10^{-5}$  Torr and the substrates were introduced using a load-lock chamber. The substrate stage was resistively heated and the substrate temperature was monitored by a thermocouple which was calibrated to the surface temperature of the substrate, measured by infrared pyrometry. The solid precursor was sublimed using a focused halogen lamp and transported to the reactor using He carrier gas. The growth atmosphere consisted of 0.5 Torr of He and 0.5 Torr of  $\text{O}_2$ . The films described in this study were grown at 725°C at a rate of 3 Å/min and with thicknesses comparable to those grown by IBSD.

The orientations of the sapphire substrates were (0 0 0 1), (1 1  $\bar{2}$  0) and (1 0  $\bar{1}$  0). These substrates were epitaxially polished by the supplier and their surface orientations are  $\pm 0.3^\circ$  to the designated plane. Prior to introduction into the vacuum chamber, all substrates were rinsed with high-purity methanol. The substrates used for growth included as-polished substrates and those which were annealed to modify their surface structures. The annealed substrates were heated to 1400°C in an oxygen atmosphere for 2–4 h, depending on their orientation. This technique has previously been described for producing faceted surface structures on sapphire substrates [13].

The ratio of Ti to oxygen and the thickness of the films were measured using Rutherford backscattering spectrometry (RBS) of 2 MeV  $^4\text{He}^+$  ions. Stoichiometric  $\text{TiO}_2$  films were grown under the conditions described here using both the IBSD and MOCVD techniques. Their crystalline structure was checked by X-ray diffraction with  $\text{Cu K}_\alpha$  radiation.

The surface morphology and roughness were examined by atomic force microscopy (AFM) under ambient conditions. AFM data from multiple locations on several samples have been examined to characterize the surface morphologies of each film type. The images shown are typical of what has been observed.

### 3. Results and discussion

#### 3.1. Heteroepitaxial structures

Table 1 shows the  $\text{TiO}_2$  film orientations grown on the sapphire substrates along with the X-ray diffraction full-width at half maximums (FWHMs) of the  $\theta$  and  $\Phi$  angles, indicating the degree of alignment of the rutile phase perpendicular to and parallel to the plane of the film. The X-ray values correspond to approximately 2000 Å thick films grown using the IBSD technique at 3 Å/min on as-polished substrates. The  $\theta$  FWHM values listed are for films grown at temperatures from 450–725°C, respectively. The  $\theta$  FWHM values decrease with increasing growth temperature for the (1 0 1) and (0 0 1) orientations and are 0.2°, 0.35° and 0.35° for the (1 0 0), (1 0 1) and (0 0 1) films grown at 725°C. The values listed for the  $\Phi$  FWHMs are for the films grown at 725°C. The  $\Phi$  FWHM of the (1 0 0) rutile film is rather large (10°) and 6 peaks are found in the  $\Phi$  scan of the 1 1 0 rutile peak. This indicates that three different

grain orientations are present in the plane of the (1 0 0) rutile film. This is due to the three-fold symmetry in the pseudo-hexagonal structure of the (0 0 0 1)  $\text{Al}_2\text{O}_3$  substrate, which is not present in the (1 0 0) tetragonal rutile structure [14]. Also shown in Table 1 are the in-plane epitaxial relationships between the film/substrate lattices and the calculated lattice mismatches between them at room temperature [1, 11]. The three grain orientations found in the (1 0 0) rutile films are aligned to the sapphire substrate with  $[0 1 0] \parallel [\bar{2} 1 1 0]$  and  $[0 0 1] \parallel [0 1 \bar{1} 0]$ . The  $\Phi$  scan of the 1 1 0 peak in the (1 0 1) rutile film has a FWHM of 0.5° and exhibits 4 peaks. The two sets of 2 peaks are most likely observed because twins are present along the (1 0 1) plane, as seen in transmission electron microscopy studies of similarly oriented films grown by MOCVD [15]. The (1 0 1) films are oriented relative to the sapphire substrate with  $[\bar{1} 0 1] \parallel [\bar{1} 1 0 0]$  and  $[0 1 0] \parallel [0 0 0 1]$ . The  $\Phi$  scan of the 1 0 1 peak of the (0 0 1) rutile film has 4 peaks with FWHMs of 1.0°. This is consistent with the (0 0 1) film being highly aligned perpendicular to and in the plane of the film with no obvious orientational defects. The alignment of the (0 0 1) rutile film on the substrate is  $[1 0 0] \parallel [1 \bar{2} 1 0]$  and  $[0 1 0] \parallel [0 0 0 1]$ .

The heteroepitaxial growth of rutile on sapphire is rather surprising due to their dissimilar structures and large lattice mismatches. The lattice mismatch in these film/substrate systems is large compared to typical heteroepitaxial semiconductor

Table 1  
Heteroepitaxy of rutile films grown on sapphire substrates

Film	Substrate	FWHM (degree)		In-plane film  substrate	Lattice mismatch (%)
		$\theta^a$	$\Phi^b$		
(1 0 0) rutile	(0 0 0 1) $\text{Al}_2\text{O}_3$	0.20	10	$[0 1 0] \parallel [\bar{2} 1 1 0]$	3.76
				$[0 0 1] \parallel [0 1 \bar{1} 0]$	7.27
(1 0 1) rutile	(1 1 $\bar{2}$ 0) $\text{Al}_2\text{O}_3$	2.85–0.35	0.5	$[\bar{1} 0 1] \parallel [\bar{1} 1 0 0]$	0.91
				$[0 1 0] \parallel [0 0 0 1]$	5.78
(0 0 1) rutile	(1 0 $\bar{1}$ 0) $\text{Al}_2\text{O}_3$	0.75–0.35	1.0	$[1 0 0] \parallel [1 \bar{2} 1 0]$	3.6
				$[0 1 0] \parallel [0 0 0 1]$	5.72

<sup>a</sup>The range of values listed for  $\theta$  correspond to the films which are approximately 2000 Å thick and are grown at temperatures 450–725°C, respectively.

<sup>b</sup>The values listed for  $\Phi$  are those corresponding to the films grown at 725°C.

films.  
to ep  
great  
factor  
preser  
and A  
compr  
ions d  
variou  
stages  
formir  
oxyge  
[11, 1:

3.2. M

The  
charac  
nesses  
morph  
proxin  
as-pol  
with a  
peratu  
(1 0 1)  
from o  
has ve  
[0 1 0]  
(RMS)  
of the  
faceted  
surface  
[ $\bar{1}$  0 1]  
which  
in this  
have si  
quite s  
prevale  
(i.e. the

Fig. 1. A  
as-polish  
rate of 3  
are (a) (1  
(a) and  
1.5 × 1.5  
(c) 400 Å

films. However, the importance of lattice mismatch to epitaxial growth is questionable when it is greater than about 2% [16]. The more important factor may be atomic matching, which seems to be present here to a much greater degree. The rutile and  $\text{Al}_2\text{O}_3$  structures can both be seen as being composed of close-packed oxygen layers with cations distributed in their octahedral sites and having various degrees of distortion. During the initial stages of rutile growth, the Ti ions can be viewed as forming an ordered lattice dependent on the oxygen pattern present on the substrate surface [11, 15].

### 3.2. Morphology development

The surface morphologies of the films have been characterized using AFM over a range of thicknesses to examine their growth mechanisms and morphologies. Fig. 1 shows AFM images of approximately 2000 Å thick rutile films grown on as-polished substrates using the IBSD technique with a growth rate of 3 Å/min and a growth temperature of 725°C. The morphologies of the (1 0 0), (1 0 1) and (0 0 1) rutile films are clearly different from one another at this thickness. The (1 0 0) film has very small features which are elongated along [0 1 0] and a surface roughness, root mean square (RMS) value, of 4–5 Å. The surface morphology of the (1 0 1) rutile films exhibits a very distinct faceted, terrace-step structure with a typical RMS surface roughness of 35 Å. The facets lie along [1 0 1]. The step height is approximately 9 Å, which is comparable to twice the lattice parameter in this direction. The (1 0 0) and (1 0 1) rutile films have significant regions of their surfaces which are quite smooth, as might be expected from their prevalence in the morphology of bulk rutile crystals (i.e. these are low surface energy planes) [17]. The

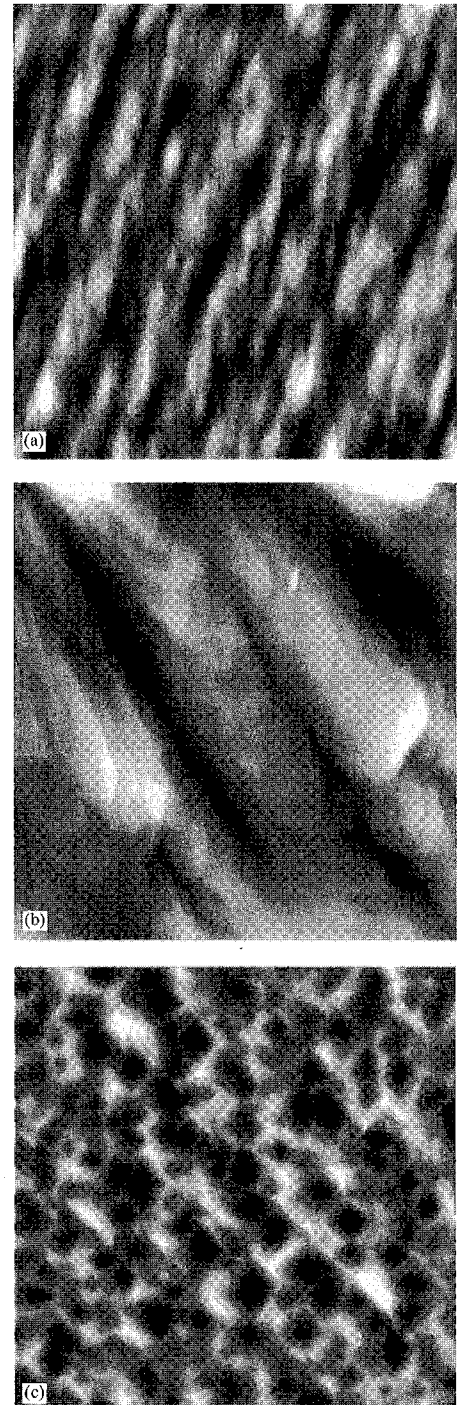


Fig. 1. AFM images of ~2000 Å thick rutile films grown on as-polished substrates using the IBSD technique with a growth rate of 3 Å/min and a growth temperature of 725°C. The images are (a) (1 0 0) rutile, (b) (1 0 1) rutile, and (c) (0 0 1) rutile. Images (a) and (b) represent a 1 × 1 μm square area. Image (c) is 1.5 × 1.5 μm. The gray scale ranges are (a) 30 Å, (b) 90 Å, and (c) 400 Å.

the plane of the  
e three-fold sym-  
structure of the  
not present in the  
[14]. Also shown  
xial relationships  
xes and the calc-  
en them at room  
rain orientations  
s are aligned to  
0]||[2 1 1 0] and  
the 1 1 0 peak in  
HM of 0.5° and  
2 peaks are most  
re present along  
mission electron  
y oriented films  
(1 0 1) films are  
re substrate with  
) 0 1]. The Φ scan  
le film has 4 peaks  
onsistent with the  
perpendicular to  
h no obvious ori-  
ent of the (0 0 1)  
0 0]||[1 2 1 0] and

rutile on sapphire  
r dissimilar struc-  
es. The lattice mis-  
systems is large  
xial semiconductor

Lattice mismatch (%)
3.76
7.27
0.91
5.78
3.6
5.72

grown at temperatures

(0 0 1) rutile film has features approximately 1000–2000 Å in size and a RMS roughness ranging between 24 and 75 Å. The (0 0 1) is not a stable rutile surface and has been observed to facet on the (1 0 1) planes upon annealing at this growth temperature [18,19]. X-ray data indicates that the edges of the features are along  $[1\ 0\ 0]$  and  $[0\ 1\ 0]$ . AFM and SEM images [1] of the (0 0 1) film surface are consistent with a (1 0 1) type faceted morphology.

The growth mechanisms of these films have been examined to help in understanding their surface morphology development. For example, Fig. 2 shows the (1 0 1) rutile film grown by IBSD on as-polished substrates at 725°C and 3 Å/min at thicknesses of 15, 100 and 700 Å. The rutile films of each orientation appear to grow via island or Volmer–Weber type growth. At 15 Å thickness, the (1 0 0), (1 0 1) (Fig. 2a) and (0 0 1) oriented films all have island-like features which are approximately 125–150 Å in diameter. The island sizes in the 100 Å thick films are larger and somewhat different depending on the film orientation. The (1 0 0) and (0 0 1) films have islands with diameters of 200–300 Å and 150–200 Å, respectively. The (1 0 1) film (Fig. 2b) has elongated islands which are approximately 200 × 500 Å. These elongated islands result most likely from the rather large difference in lattice mismatch between the two axes in the plane of the film (Table 1). The elongated facets in the thicker (1 0 1) film (Fig. 1b) are along the  $[\bar{1}\ 0\ 1]$  direction, or the direction of smallest mismatch. TEM studies of (1 0 1) films grown on (1 1  $\bar{2}$  0) Al<sub>2</sub>O<sub>3</sub> substrates by MOCVD have a coherent interface along  $[\bar{1}\ 0\ 1]$  and a periodic (~90 Å spacing) dislocation structure along  $[0\ 1\ 0]$  [15]. The thicker (1 0 0) film (Fig. 1a) also has elongated features along the direction of smallest lattice mismatch,  $[0\ 1\ 0]$ . Table 2 shows the RMS roughnesses of the 15 and 100 Å thick films. Their RMS roughnesses correlate with their lattice mismatches,

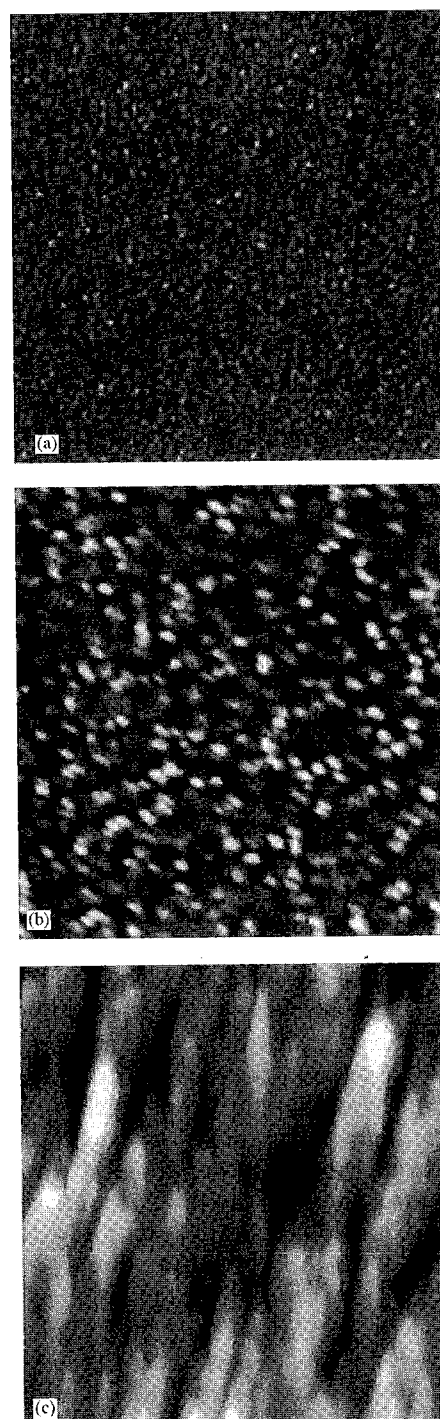


Fig. 2. AFM images of (1 0 1) rutile films grown with conditions comparable to those of the films in Fig. 1. The images are of films which are (a) 15 Å, (b) 100 Å, and (c) 700 Å thick. Each image represents a 1 × 1 μm square area. The gray scale ranges are (a) 20 Å, (b) 30 Å, and (c) 50 Å.

Table 2  
RMS roughn

Film<sup>a</sup>

(1 0 0) rutile  
(1 0 1) rutile  
(0 0 1) rutile

<sup>a</sup>The growth

shown in T  
inversely re  
of their sa  
ships are co  
growth me  
deposition.  
tems are 1  
maximizing  
growth wh  
the substra

The incr  
rutile films  
grown at 5  
structures  
growth tem  
size appear  
on thickne  
epitaxial se  
gated [12,  
thickness n  
coarsening  
cussion of  
[21].

By the  
3 Å/min re  
morpholog  
minimize th  
by the time  
gated, facet  
2000 Å thic  
tures which  
bulk rutile  
films have ;  
perature fo  
were stable.

Table 2  
RMS roughness values for 15 and 100 Å thick rutile films on polished and annealed substrates

Film <sup>a</sup>	Substrate	Polished substrates roughness RMS (Å)		Annealed substrates roughness RMS (Å)	
		15 Å thick	100 Å thick	15 Å thick	100 Å thick
(1 0 0) rutile	(0 0 0 1) Al <sub>2</sub> O <sub>3</sub>	3.5	8.5	6.3	12.5
(1 0 1) rutile	(1 1 $\bar{2}$ 0) Al <sub>2</sub> O <sub>3</sub>	2.4	5.8	3.4	4.6
(0 0 1) rutile	(1 0 $\bar{1}$ 0) Al <sub>2</sub> O <sub>3</sub>	2.2	6.7	6.2	39

<sup>a</sup>The growth conditions of these films are comparable to those for the films shown in Figs. 1 and 2.

shown in Table 1. Their RMS roughnesses are also inversely related to the calculated surface energies of their sapphire substrates [20]. These relationships are consistent with a three-dimensional island growth mechanism, during the early stages of film deposition. The energies of the film/substrate systems are minimized under these conditions by maximizing the three-dimensional character of growth when the lattice mismatch is large and/or the substrate surface energy is small.

The increase in island size with thickness of the rutile films has been examined using (1 0 1) films grown at 550°C. In these films, the large faceted structures do not form as readily as when the growth temperature is 725°C. The increase in island size appears to follow a power law dependence (0.4) on thickness, similar to other types of heteroepitaxial semiconductor and oxide films investigated [12, 21]. The increase in island size with thickness may be attributed to a coalescence and coarsening processes [12, 22]. For further discussion of this aspect of growth, please see Ref. [21].

By the time the films grown at 725°C and 3 Å/min reach a thickness of 700–2000 Å, their morphologies are evolving toward structures which minimize their surface energies. As seen in Fig. 2c, by the time the (1 0 1) film is 700 Å thick, an elongated, faceted surface structure has developed. The 2000 Å thick films shown in Fig. 1 have facet structures which appear to mimic the facets found on bulk rutile crystal surfaces [17]. The 2000 Å thick films have also been annealed at the growth temperature for 12 h and their surface morphologies were stable.

The results on these films suggest a process of morphology development which is clearly influenced by their three-dimensional island growth mechanism. At the early stages of growth, the islands are nucleated on the substrate surface and grow in a coalescence and coarsening process. As the thickness of the films increases, they develop morphologies and facets which minimize their surface energies.

### 3.3. Substrate surface effects

The films described above were grown on polished sapphire substrates with RMS roughnesses of 0.8–1.1 Å. The (1 0  $\bar{1}$  0) sapphire surface is essentially featureless in the AFM. However, the (0 0 0 1) and (1 1  $\bar{2}$  0) substrates have a terrace-step structure with terraces which are approximately 650 and 1000 Å wide, respectively.

Substrates were annealed so that the effects of different substrate surface structures on subsequent growth morphologies could be examined. The annealed (0 0 0 1) and (1 1  $\bar{2}$  0) sapphire substrates had very well developed terrace-step structures on their surfaces. The terrace widths ranged in size from 750–3000 Å, with an average of 2400 Å, on the (0 0 0 1) substrate. On (1 1  $\bar{2}$  0), the facet-edged terraces were approximately 1000–7000 Å wide, with an average of 4000 Å. The terraces, between the steps, on both the (0 0 0 1) and (1 1  $\bar{2}$  0) substrates were relatively smooth, with RMS roughness of 2.8 and 3.6 Å, respectively. The step height on the (0 0 0 1) substrates was observed to be 9 Å, as previously seen in other annealing studies [13]. The

(1 1  $\bar{2}$  0) steps were 14 Å high, which is comparable to three times the lattice parameter in this direction. On (0 0 0 1) and (1 1  $\bar{2}$  0) annealed substrates, a coalescence or coarsening of the surface steps present after polishing has occurred. The (1 0  $\bar{1}$  0) substrate surface has a hill-and-valley type of structure. The formation of this structure is described in detail, elsewhere [13]. The facets are reported to lie along [1  $\bar{2}$  1 0] with (1 0  $\bar{1}$  1) planes. The facet widths were approximately 1000 Å. The facet heights ranged from 50 to 200 Å, with the average observed to be 125–150 Å.

The morphologies of the films grown on the annealed substrates were examined during different stages of growth and compared to those grown on the as-polished substrates. The sizes of the islands observed in the 15 and 100 Å thick films are comparable to those found on the as-polished substrates. However, the RMS roughnesses, shown in Table 2, were significantly larger, except for the 100 Å thick (1 0 1) rutile film. The increased roughnesses may be due to more three-dimensional type growth on the annealed substrates, having reduced surface energies. The roughnesses of the (0 0 1) rutile films are larger than expected by comparison to the other films, most likely due to their growth on the (1 0  $\bar{1}$  1) faceted substrate.

Fig. 3 shows the morphologies of 2000 Å thick rutile films grown on the annealed substrates using the IBSD technique at 725°C and 3 Å/min (the same conditions used for the films shown in Figs. 1 and 2). The (1 0 0) rutile film grown on the annealed substrate has a very faceted surface structure with a RMS roughness of approximately 104 Å. This is quite different from the relatively flat and featureless morphology of films grown on an as-polished (0 0 0 1) sapphire (Fig. 1a). The morphology of the (1 0 1) rutile film grown on the annealed substrate was comparable to that of the film grown on the as-polished substrate, seen in Fig. 1b. The (0 0 1) rutile film has a very different morphology when grown on the faceted (1 0  $\bar{1}$  0) substrate. Elongated features are present and the film has a RMS roughness of 90 Å. Both the (1 0 0) and (0 0 1) films are much rougher when grown on the annealed substrates. In addition, the  $\theta$  FWHMs of these films are approximately 0.10°–0.15° wider than of films grown on the as-polished substrates. These results

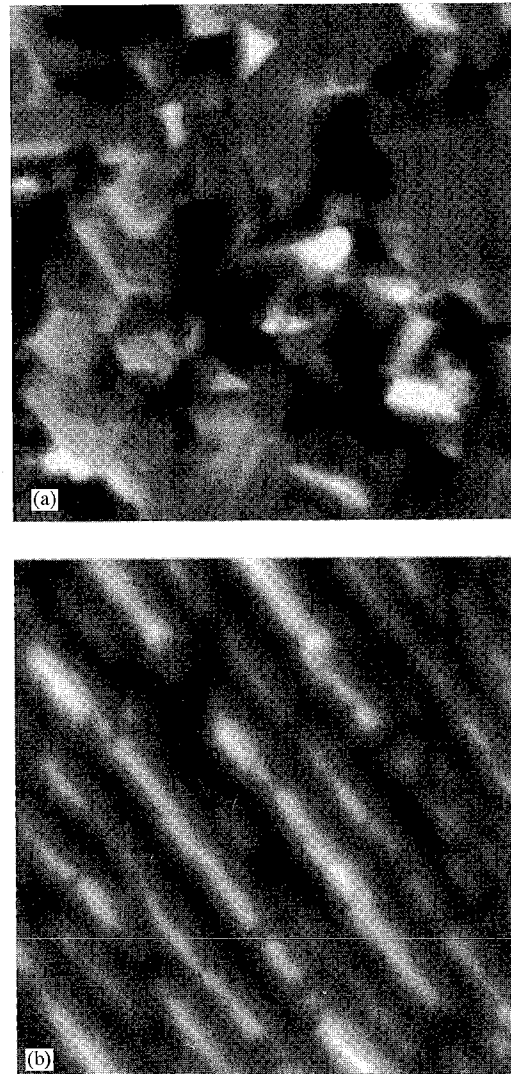


Fig. 3. AFM images of  $\sim 2000$  Å thick rutile films grown on annealed substrates with conditions comparable to those of the films in Fig. 1. The images are (a) (1 0 0) rutile and (b) (0 0 1) rutile. Each image represents a  $1 \times 1$   $\mu\text{m}$  square area and has a gray scale range of 500 Å.

suggest that rougher and slightly less crystallographically aligned (1 0 0) and (0 0 1) rutile films are produced by the more three-dimensional type growth found during the early stages of deposition on the annealed substrates. It is unclear as to why exactly the (1 0 1) film morphology is not affected.

### 3.4. Growth

The effect the surface n to the (1 0 1) in observing tures. The (1 strates using 7 Å/min hav Fig. 1b (gro steps which a present para [1 0 1]. This creases in th can change present.

The effect sity during th detail elsewh density of isl creasing sub: dependence i cleation or a face morphol grown using 550°C does n ture shown : morphology found in Ref 100 Å thick grown at 72 controlling tl tures of the tl dependence a

### 3.5. IBSD ver

The growth rutile films gr niques using pared to exa chemical dep tures develop in thin (15 Å tures increase as described a ever, the surfa films are quite



### 3.4. Growth rate and temperature dependence

The effects of growth rate and temperature on the surface morphologies are discussed with respect to the (1 0 1) rutile films because of the relative ease in observing changes in their terrace-step structures. The (1 0 1) films grown on as-polished substrates using the IBSD technique at 725°C and 7 Å/min have a terrace-step structure as seen in Fig. 1b (grown at 3 Å/min), but a large number of steps which are approximately 400–500 Å wide are present parallel to the length of the terraces, along  $[\bar{1} 0 1]$ . This indicates that relatively small increases in the growth rate, at these very low rates, can change the details of the surface structures present.

The effect of growth temperature on island density during the early stages of growth is discussed in detail elsewhere [21]. The data suggest that the density of islands decreases exponentially with increasing substrate temperature. This temperature dependence is consistent with homogeneous nucleation or a diffusion controlled process. The surface morphology of a 2000 Å thick (1 0 1) rutile film grown using the IBSD technique at 3 Å/min and 550°C does not have the distinct terrace-step structure shown in Fig. 1b. An image of the surface morphology of the film grown at 550°C can be found in Ref. [21]. It has features similar to the 100 Å thick film shown in Fig. 2b, which was grown at 725°C. This suggests that the process controlling the development of the surface structures of the thicker films has a strong temperature dependence as well.

### 3.5. IBSD versus MOCVD

The growth morphologies of (1 0 0) and (1 0 1) rutile films grown by the IBSD and MOCVD techniques using similar conditions have been compared to examine the effects of a physical versus chemical deposition process on the surface structures developed. Island-like features are observed in thin (15 Å thick) MOCVD films and these features increase in size with the thickness of the films, as described above for films grown by IBSD. However, the surface morphologies of thicker MOCVD films are quite different from the IBSD films. Fig. 4

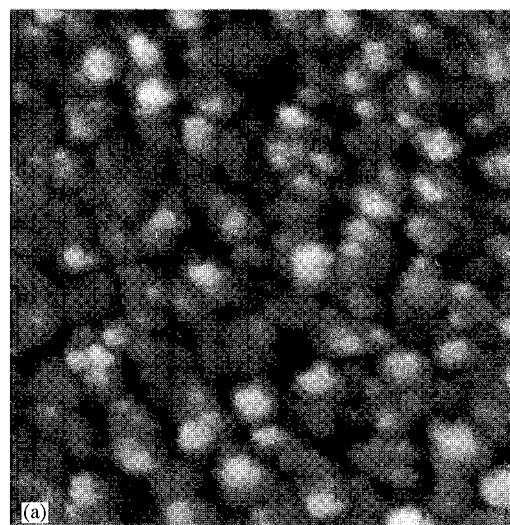
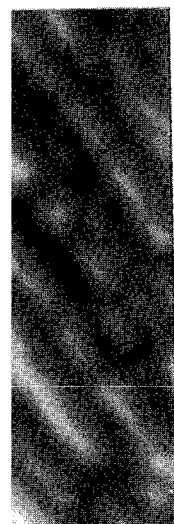
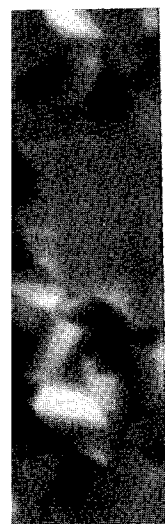


Fig. 4. AFM image of a  $\sim 2000$  Å thick (1 0 1) rutile film grown using the MOCVD technique with a growth rate of 3 Å/min and a growth temperature of 725°C. The image represents a  $1 \times 1$   $\mu\text{m}$  square area and has a gray scale range of 300 Å.

shows the surface morphology of an approximately 2000 Å thick, (1 0 1) rutile film grown by the MOCVD technique at the same temperature, growth rate and oxygen partial pressure ( $P_{\text{O}_2}/P_{\text{total}}$ ) as those used for the IBSD film shown in Fig. 1b. The MOCVD film does not exhibit the terrace-step surface morphology seen on the IBSD film. The MOCVD film has approximately 1000 Å features and a RMS surface roughness of 56 Å. The (1 0 0) rutile film grown by the MOCVD technique has a surface structure which is similar to the (1 0 1) film shown in Fig. 4 and has a surface roughness of 65 Å. This is quite different from the (1 0 0) IBSD film shown in Fig. 1a, with a RMS surface roughness of 4–5 Å. The precise reasons for the differences in the surface morphologies are not known at this time. Both thermodynamic and kinetic effects may be important. The growing film surface is in contact with the same partial pressure of  $\text{O}_2$ , but a different atmosphere ( $\text{He}/\text{O}_2$ ) and a higher total pressure in the MOCVD process. Also, during the chemical deposition process the  $\text{Ti}(\text{TMHD})_3$  molecules must decompose prior to the diffusion of Ti ions on the surface of the growing film. In addition, more energetic species may be expected at the



rutile films grown on a substrate comparable to those of the (1 0 1) rutile and (0 0 1) rutile films. The image represents a  $1 \times 1$   $\mu\text{m}$  square area and has a gray scale range of 300 Å.

ly less crystalline (1 0 1) rutile films are dimensional type. The growth rate and temperature are unclear as to why the surface morphology is not affected.



surface of the growing IBSD film due to the nature of the technique. The MOCVD film in Fig. 4 has a morphology which is similar to the (1 0 1) IBSD films grown at 550°C [21]. This suggests that the evolution of the surface morphologies of the MOCVD films is limited by kinetic effects.

#### 4. Conclusions

The growth morphologies of (1 0 0), (1 0 1) and (0 0 1) rutile films grown on sapphire substrates by the IBSD technique have been examined as a function of film/substrate orientation, film thickness, substrate surface preparation, growth rate and growth temperature. The results are consistent with the following probable path of growth morphology evolution. The rutile films of each orientation grow via island (Volmer–Weber) type growth. At the early stages of growth ( $\leq 100$  Å), the RMS roughnesses of the films, grown on as-polished substrates at 725°C and 3 Å/min, are correlated to their lattice mismatches and inversely related to the calculated surface energies of their sapphire substrates. The islands then grow in a coalescence and coarsening process, which exhibits a power law dependence on film thickness. At these stages, the morphologies are clearly influenced by their growth mechanisms. As the thickness of the films increases ( $\geq 700$  Å), they develop morphologies which minimize their surface energies and eventually attain facet structures that mimic the facets found on bulk rutile crystals and are stable with respect to annealing. The evolution of the morphologies of the films can be modified by changes in the growth conditions, such as growth rate, growth temperature or growth technique, which affect the diffusion processes occurring during growth. Relatively small increases in the growth rate, at very low rates, are observed to change the details of the surface structures present. The morphologies observed on films grown over a range of temperatures indicate that the processes controlling their development have a strong temperature dependence at all stages. Comparisons made between (1 0 0) and (1 0 1) rutile films grown by the IBSD and MOCVD techniques under similar conditions have shown that the MOCVD films have morphologies which are similar to IBSD films

of the same thickness, but grown at lower temperatures. Rougher and slightly less crystallographically aligned (1 0 0) and (0 0 1) rutile films result from more three-dimensional type growth on annealed sapphire substrates, indicating that the condition of the substrate surface is also an important factor.

#### Acknowledgements

The authors would like to thank G.A. Wilson and D.R. Burgess for experimental assistance. Portions of this material are based upon work supported under a National Science Foundation Graduate Fellowship and G.S. Rohrer acknowledges support from the National Science Foundation under a YIA grant DMR-9458005. RBS measurements were done using the facility at the Laboratory for Research on the Structure of Matter at the University of Pennsylvania. The contribution of the National Institute of Standards and Technology is not subject to copyright.

#### References

- [1] P.A. Morris Hotsenpiller, G.A. Wilson, A. Roshko, J.B. Rothman and G.S. Rohrer, *J. Crystal Growth* 166 (1996) 779.
- [2] R.N. Ghoshtagore and A.J. Noreika, *J. Electrochem. Soc.* 117 (1970) 1310.
- [3] Y. Kumashiro, Y. Kinoshita, Y. Takaoka and S. Murasawa, *J. Ceram. Soc. Jpn.* 101 (1993) 514.
- [4] D.R. Burgess, P.A. Morris Hotsenpiller, T.J. Anderson and J.L. Hohman, *J. Crystal Growth* 166 (1996) 763.
- [5] J.C. Parker, H.L.M. Chang, J.J. Xu and D.J. Lam, *Mater. Res. Soc. Symp.* 168 (1990) 337.
- [6] H.L.M. Chang, H. You, J. Guo and D.J. Lam, *Appl. Surf. Sci.* 48/49 (1991) 12.
- [7] Y. Gao, K.L. Merkle, H.L.M. Chang, T.J. Zhang and D.J. Lam, *Mater. Res. Soc. Symp.* 221 (1991) 59.
- [8] S. Chen, M.G. Mason, H.J. Gysling, G.R. Paz-Pujalt, T.N. Blanton, T. Castro, K.M. Chen, C.P. Fitorie, W.L. Gladfelter, A. Franciosi, P.I. Cohen and J.G. Evans, *J. Vac. Sci. Technol. A* 11 (1993) 2419.
- [9] K. Fukushima, I. Yamada and T. Takagi, *J. Appl. Phys.* 58 (1985) 4146.
- [10] K. Fukushima and I. Yamada, *Surf. Coatings Technol.* 51 (1992) 197.
- [11] K. Fukushima, G.H. Takaoka and I. Yamada, *Jpn. J. Appl. Phys.* 32 (1993) 3561.

at lower temper-  
crystallographi-  
tile films result  
growth on aning  
that the conso  
an important

nk G.A. Wilson  
l assistance. Por-  
upon work sup-  
nce Foundation  
Rohrer acknow-  
Science Founda-  
R-9458005. RBS  
he facility at the  
structure of Mat-  
nia. The contribu-  
f Standards and  
yright.

lson, A. Roshko, J.B.  
al Growth 166 (1996)

i, J. Electrochem. Soc.

l. Takaoka and S.  
(1993) 514.

ller, T.J. Anderson and  
6 (1996) 763.

and D.J. Lam, Mater.

l D.J. Lam, Appl. Surf.

ang, T.J. Zhang and  
221 (1991) 59.

, G.R. Paz-Pujalt, T.N.  
Fitorie, W.L. Gladfel-

G. Evans, J. Vac. Sci.

akagi, J. Appl. Phys. 58

f. Coatings Technol. 51

nd I. Yamada, Jpn. J.

[12] Mater. Res. Soc. Symp. 399 (1996).

[13] J.R. Heffelfinger, M.W. Bench and C.B. Carter, Mater. Res. Soc. Symp. 399 (1996) 263.

[14] H.L.M. Chang, T.J. Zhang, H. Zhang, J. Guo, H.K. Kim and D.J. Lam, J. Mater. Res. 8 (1993) 2634.

[15] H.L.M. Chang, H. You, Y. Gao, J. Guo, C.M. Foster, R.P. Chiarello, T.J. Zhang and D.J. Lam, J. Mater. Res. 7 (1992) 2495.

[16] K.R. Sarma, P.J. Shlichta, W.R. Wilcox and R.A. Lefever, J. Crystal Growth 174 (1997) 487.

[17] J.D. Dana and E.S. Dana, The System of Mineralogy, (Wiley, New York, 1944) p. 554.

[18] L.E. Firment, Surf. Sci. 116 (1982) 205.

[19] R.L. Kurtz, Surf. Sci. 177 (1986) 526.

[20] W.C. Mackrodt, J. Chem. Soc. Faraday Trans. 85 (1989) 541.

[21] A. Roshko, F.J.B. Stork, D.A. Rudman, D.J. Aldrich, P.A. Morris Hotsenpiller, J. Crystal Growth 174 (1997) 398.

[22] B. Lewis and J.C. Anderson, Nucleation and Growth of Thin Films (Academic Press, London, 1978).